Electronic Supplementary Information (ESI)

Highly stable 8-hydroxyquinolinate-based metal-organic framework as a selective fluorescence sensor for Fe^{3+}, $Cr_2O_7^{2-}$ and nitroaromatic explosives

Quan Sun,† Kun Yang,† Wenna Ma, Liyan Zhang and Guozan Yuan*

School of Chemistry and Chemical Engineering, Institute of Materials Science and Engineering, Anhui University of Technology, Maanshan, 243032, China.

Corresponding Author E-mail: guozan@ahut.edu.cn

†These authors contributed equally to this work.

Table of Contents

Table S1. Crystal data and structure refinement for complex **1**.

Complex	**1**
Formula	$C_{26}H_{25}NO_8Zn$
F_w	543.09
cryst syst	Tetragonal
space group	$P4_3$
a (Å)	16.3284(10)
b (Å)	16.3284(10)
c (Å)	10.9888(10)
α (deg)	90
β (deg)	90
γ (deg)	90
V (Å^3)	2160.1(2)
Z	4
D_c (g.cm^{-3})	1.210
F(000)	1084
μ (mm^{-1})	1.535
T (K)	173
reflns/unique	40497/5570
R_{int}	0.0540
data/restraints/params	5570/3/300
GOF on F^2	1.100
R_1, wR_2 ($I > 2\sigma(I)$)	0.0735, 0.1980
R_1, wR_2 (all data)	0.0753, 0.2013
largest diff. peak and hole (e.Å^{-3})	1.013, -0.765

Table S2. Selected bond lengths [Å] and angles [º] for **1**.

Zn(1)-O(1)	2.231(9)	N(1)-Zn(1)-O(2)#1	136.7(3)
Zn(1)-N(1)	2.297(8)	N(1)-Zn(1)-O(4)#2	127.2(3)
Zn(1)-O(2)#1	2.473(8)	N(1)-Zn(1)-O(5)#2	91.7(3)
Zn(1)-O(3)#1	2.258(8)	O(3)#1-Zn(1)-N(1)	112.4(3)
Zn(1)-O(4)#2	2.321(7)	O(3)#1-Zn(1)-O(2)#1	56.1(3)
Zn(1)-O(5)#2	2.349(8)	O(3)#1-Zn(1)-O(4)#2	110.7(3)
O(1)-Zn(1)-N(1)	74.3(3)	O(3)#1-Zn(1)-O(5)#2	95.0(3)
O(1)-Zn(1)-O(2)#1	88.6(3)	O(4)#2-Zn(1)-O(2)#1	92.9(3)
O(1)-Zn(1)-O(3)#1	136.3(3)	O(4)#2-Zn(1)-O(5)#2	55.5(3)
O(1)-Zn(1)-O(4)#2	94.4(3)	O(5)#2-Zn(1)-O(2)#1	128.5(3)
O(1)-Zn(1)-O(5)#2	128.6(3)	C(7)-O(1)-Zn(1)	114.9(7)

Symmetry transformations used to generate equivalent atoms:

#1 -y+1, x+1, z+3/4 #2 -y+1, x, z+3/4

Fig. S1 (a) ^{1}H and (b) ^{13}C NMR spectra of H_2L (The peaks at 3.36 in ^{1}H NMR and 66.8 in ^{13}C NMR can be easily assigned to the signals of 1,4-dioxane) .

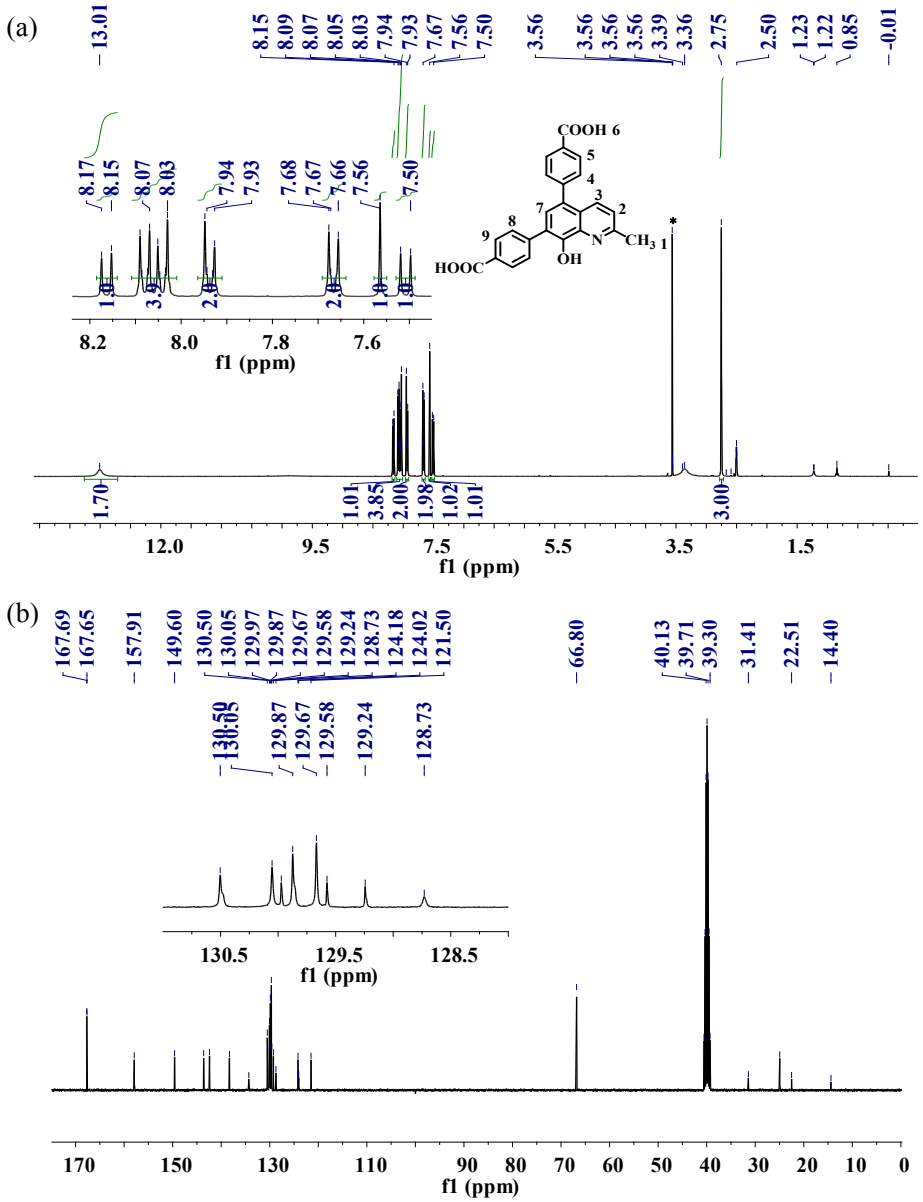

Fig. S2 HR-MS spectroscopy of H_2L.

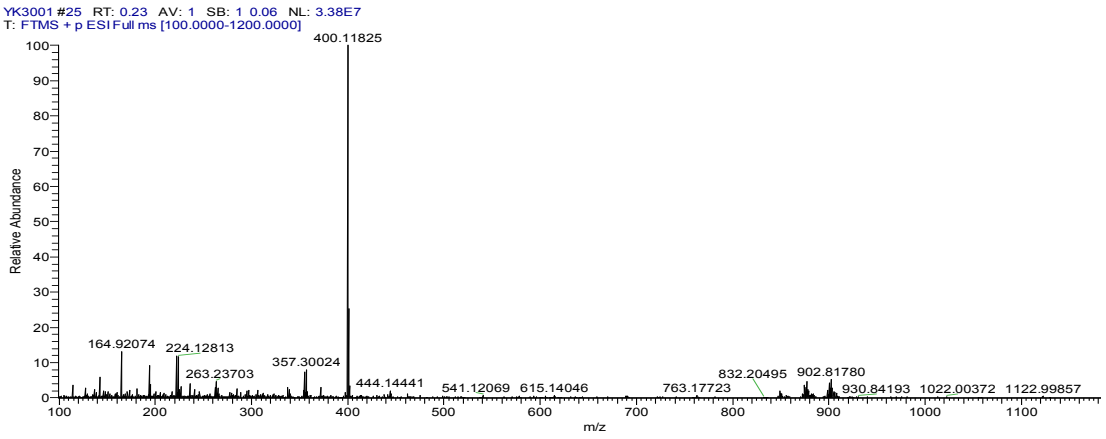

Fig. S3 View of the asymmetric unit of **1.**

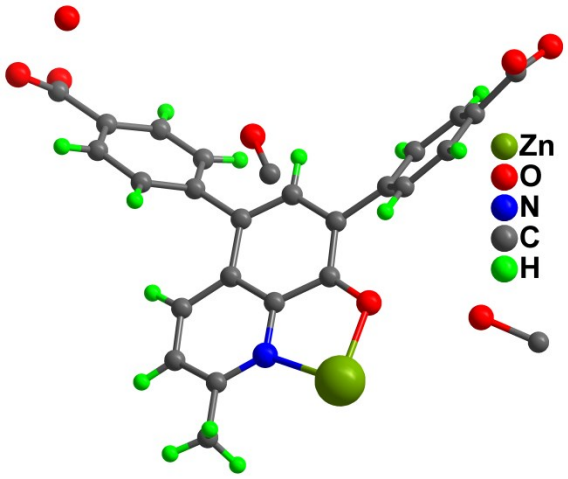

Fig. S4 The space-filling mode of a large cage in **1** fabricated by nine Zn(II) atoms and nine L.

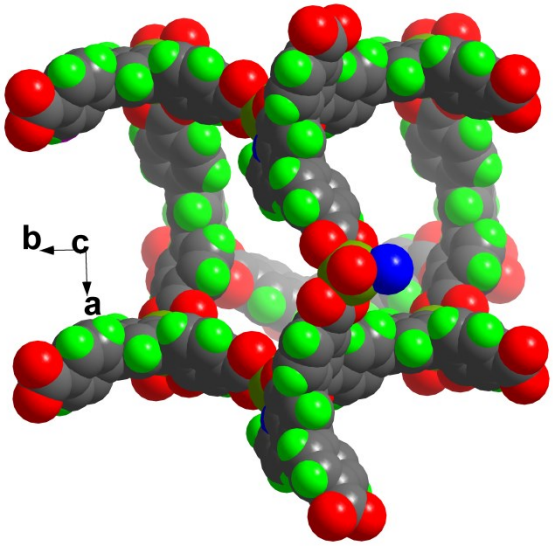

Fig. S5 A right-handed 4_3 helix in **1** with a pitch of 32.966(3) Å.

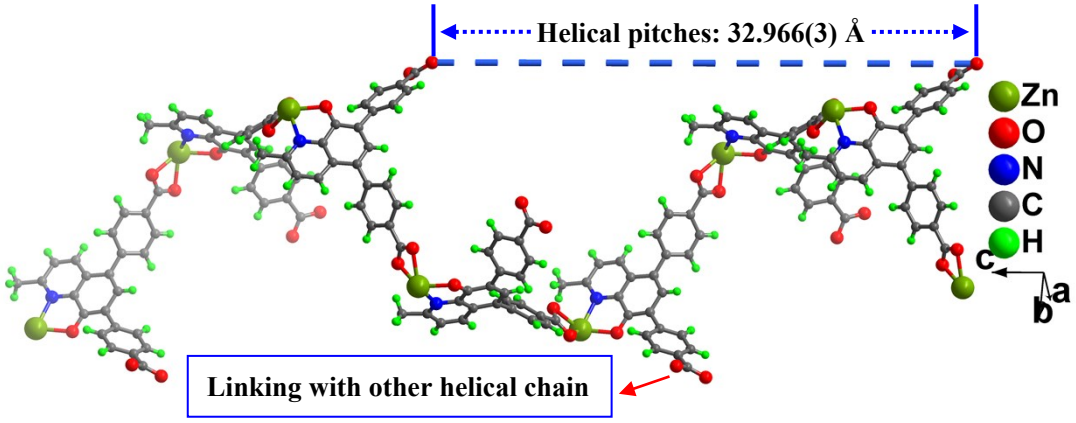

Fig. S6 Three infinite four-fold helical chains in **1** are arranged in parallel.

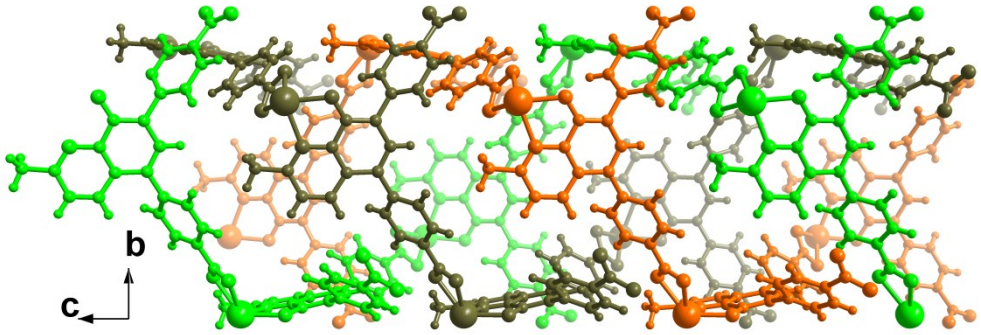

Fig. S7 Porous framework **1** possesses two different 1D channels.

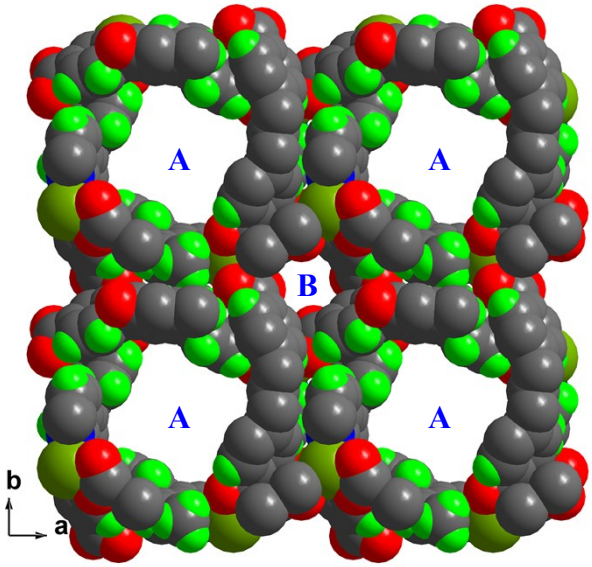

Fig. S8 The channels in **1** are occupied by guest MeOH and H_2O molecules.

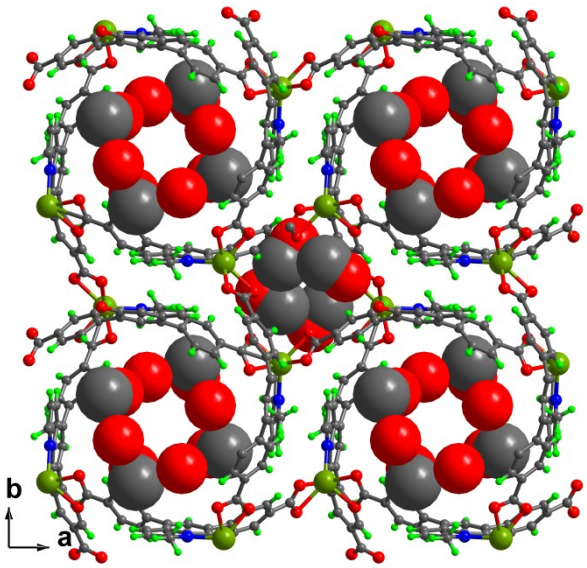

Fig. S9 FTIR spectrum of complex **1.**

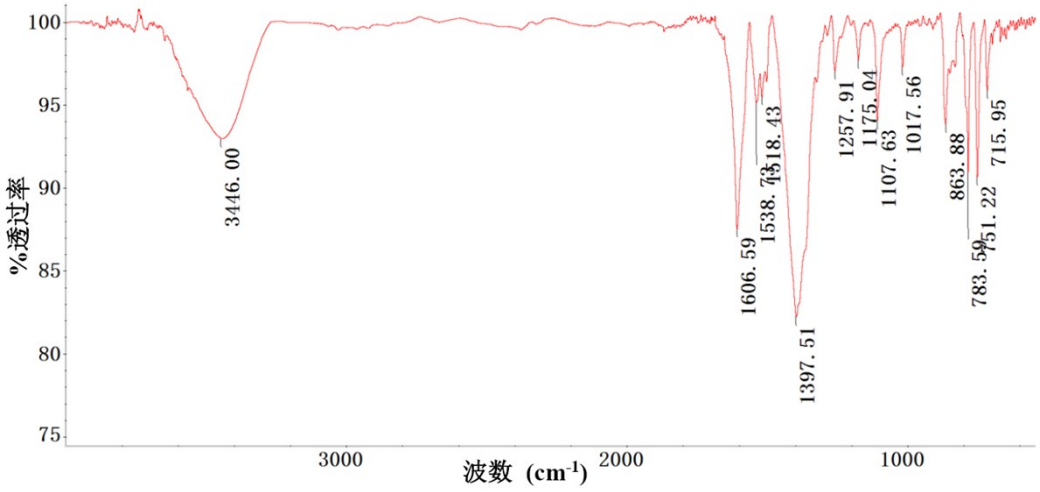

Fig. S10 TGA curve for complex **1**.

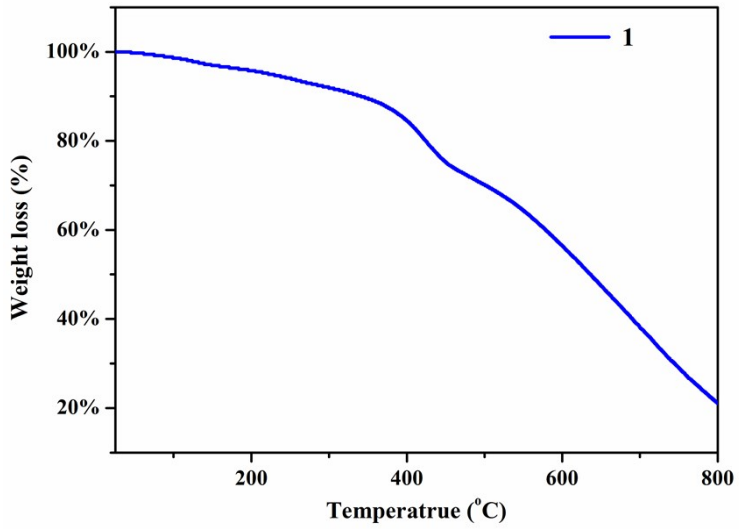

Fig. S11 Fluorescence spectra of free ligand H_2L and complex **1** in the solid state (λ_{ex} = 350 nm).

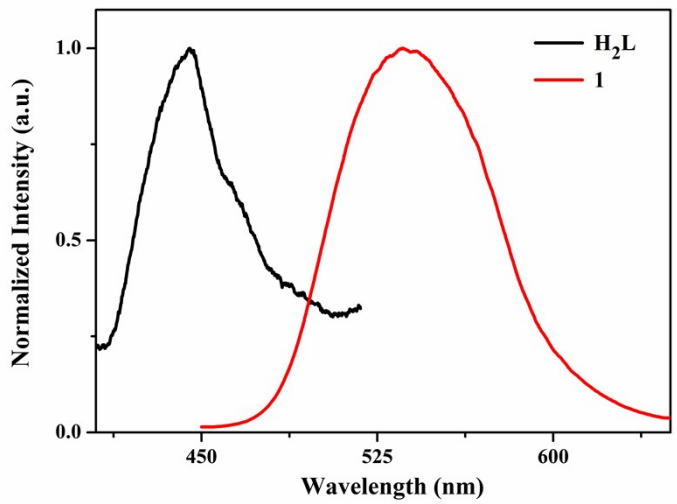

Fig. S12 Fluorescence intensities of **1** soaked in the $M(NO_3)_x$ or $FeSO_4$ aqueous solutions.

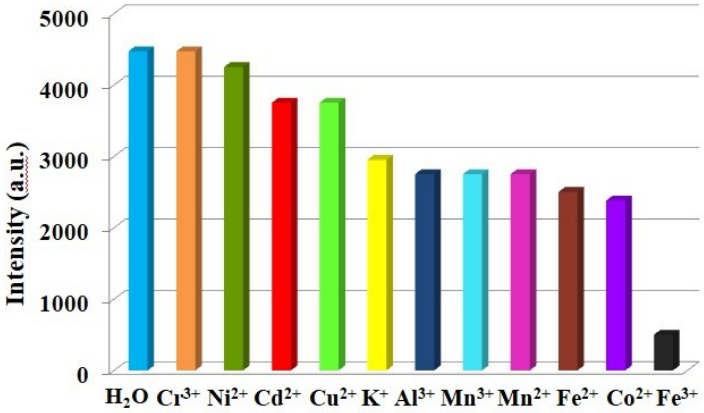

Fig. S13 Upon addition of different Ln^{3+} cations, fluorescence spectra (a) and intensity (b) of suspension of **1** (λ_{ex} = 350 nm).

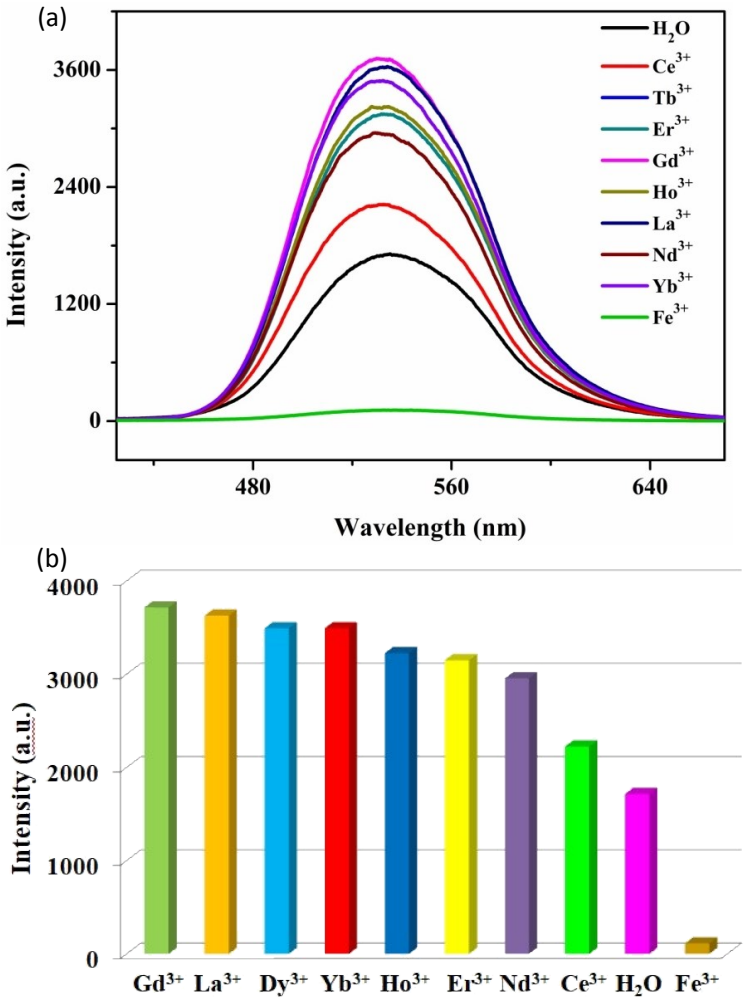

Fig. S14 Fluorescence intensities of **1** immersed in the individual aqueous solutions of $Ln(NO_3)_3$ (1 mM; red color) and mixed metal ions including Fe^{3+} ion (1 mM; blue color) under an excitation of 350 nm.

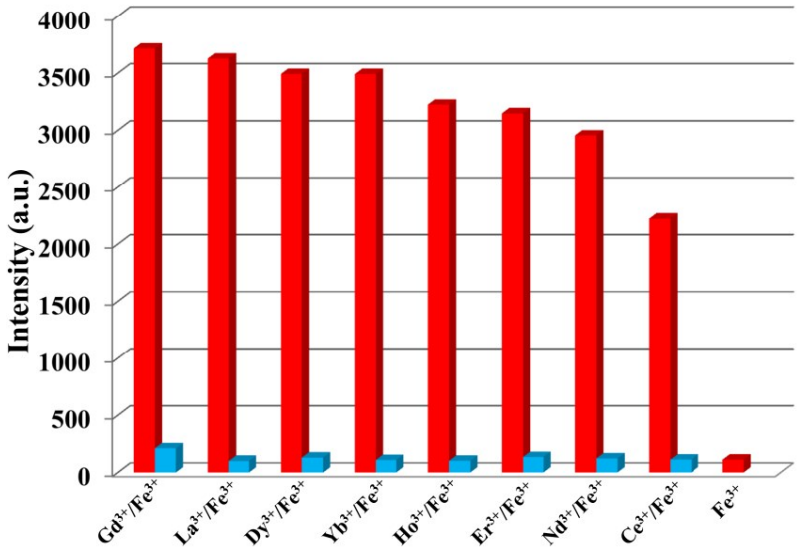

Fig. S15 (a) Quenching efficiency (%) of **1** with different concentrations of $Fe(NO_3)_3$ based on the equation: Quenching efficiency (%) = $(I_0 - I)/I_0 \times 100\%$; (b)The recyclability test for sensing Fe^{3+}. Emission intensity of **1**, Fe@**1**, @**1**, 2nd, 5th.

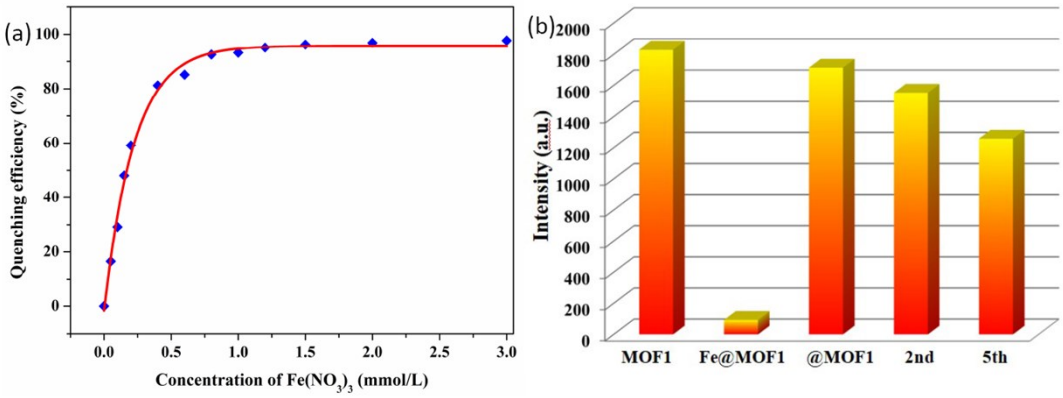

The recyclability test: Emission intensity of **1**, Fe@**1**, @**1**, 2nd, 5th. (Noting: Fe@**1** sample dispersed in an iron nitrate solution sonicated for 30 minutes; @**1** is supersonic ultrasound, centrifuged and washed with distilled water until the solution is colorless; 2nd is the repeat experiment with the same batch of samples at second times; 5th is the fifth repeated test with the same sample.

Fig. S16 The UV−vis absorption spectra of aqueous solutions containing various mental ions ($M(NO_3)_x$ or $FeSO_4$) with the same volume of 1 mmol·L^{-1}, the excitation spectrum and the absorption spectra of **1** (2 mg) dispersed in water (2 mL); (b) The UV−vis absorption spectra of Fe^{3+} with increasing concentrations.

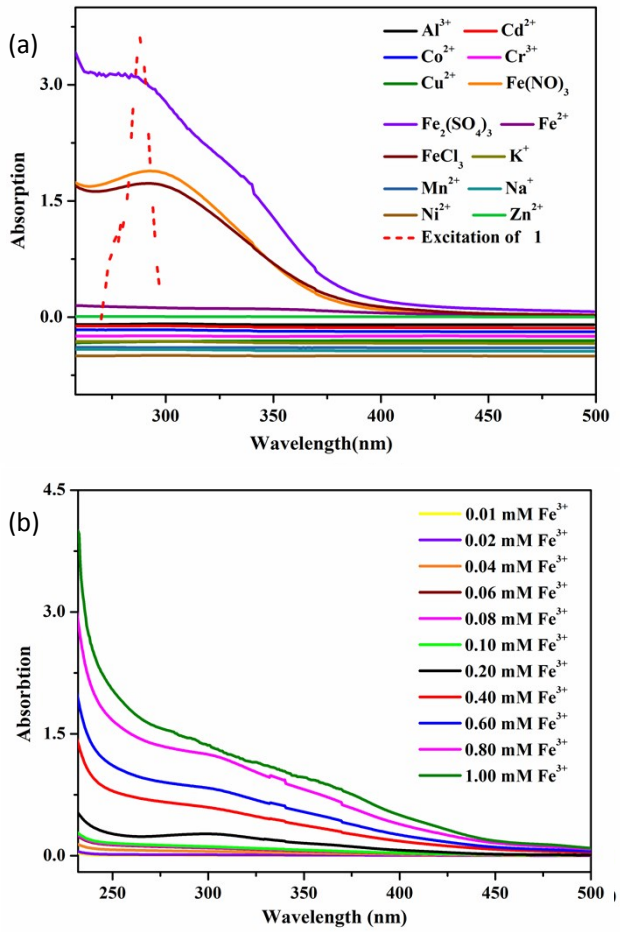

Fig. S17 Fluorescence spectra of **1** immersed in aqueous solution of different anions (1.0 mM), λ_{ex} = 350 nm.

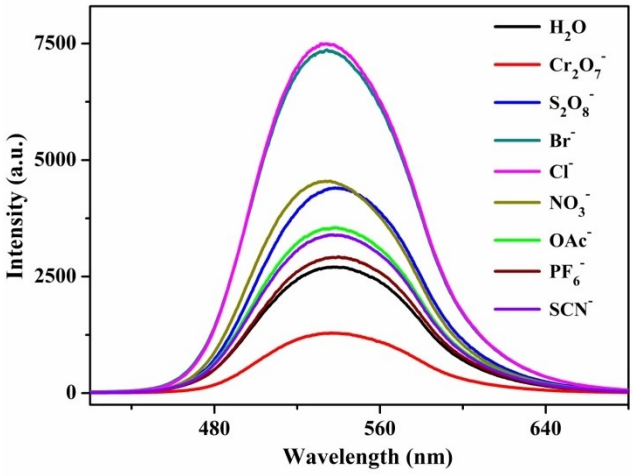

Fig. S18 Fluorescence spectra (a) and intensity (b) of suspension of **1**immersed in different organic solvents (λ_{ex} = 350 nm).

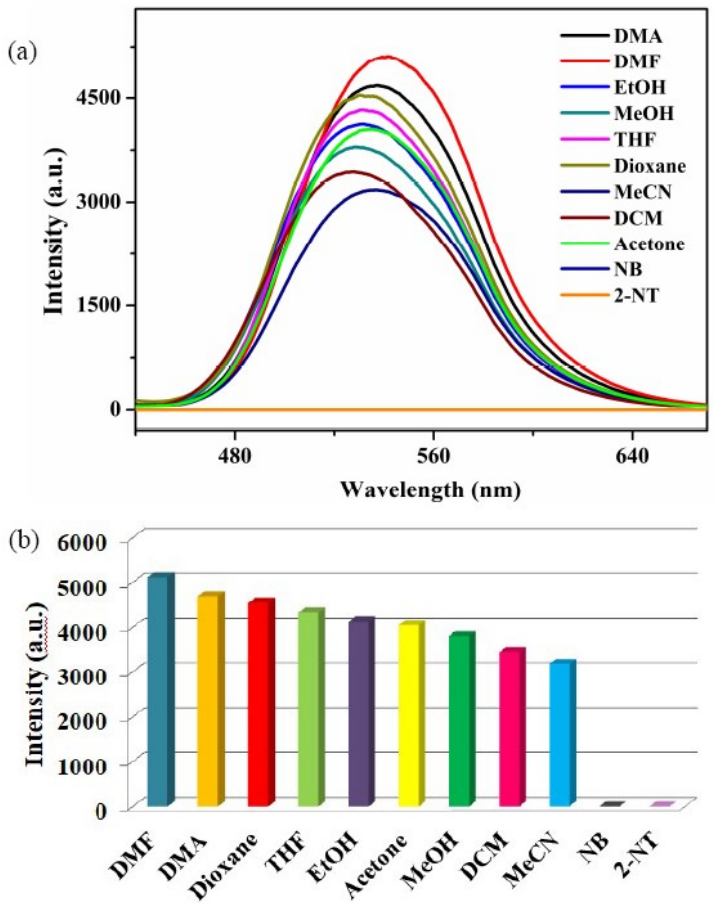

Fig. S19 PXRD patterns of simulated, as-synthesized, and recovered **1** after five cycles for NACs sensing.

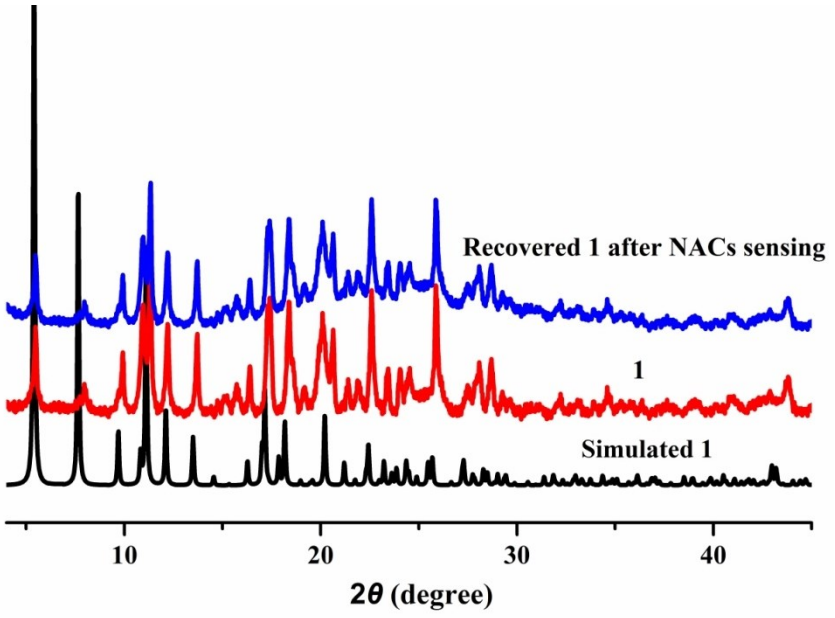

Fig. S20 The recyclability investigation of **1** for sensing NACs (a: NB; b: 2-NT; c: TNT; d: TNP).